© 2020. Published by The Company of Biologists Ltd | Journal of Experimental Biology (2020) 223, jeb230896. doi:10.1242/jeb.230896

SHORT COMMUNICATION

The myodural bridge of the American alligator (*Alligator mississippiensis*) alters CSF flow

Bruce A. Young[1,*], James Adams[1], Jonathan M. Beary[2], Kent-Andre Mardal[3], Robert Schneider[4] and Tatyana Kondrashova[4]

ABSTRACT

Disorders of the volume, pressure or circulation of the cerebrospinal fluid (CSF) lead to disease states in both newborns and adults; despite this significance, there is uncertainty regarding the basic mechanics of the CSF. The suboccipital muscles connect to the dura surrounding the spinal cord, forming a complex termed the 'myodural bridge'. This study tests the hypothesis that the myodural bridge functions to alter the CSF circulation. The suboccipital muscles of American alligators were surgically exposed and electrically stimulated simultaneously with direct recordings of CSF pressure and flow. Contraction of the suboccipital muscles significantly changed both CSF flow and pressure. By demonstrating another influence on CSF circulation and pulsatility, the present study increases our understanding of the mechanics underlying the movement of the CSF.

KEY WORDS: Meninges, Crocodilia, Neuroscience, Fluid mechanics, Skeletal muscle

INTRODUCTION

Recent breakthroughs in neuroscience have demonstrated that neurodegenerative diseases, and Alzheimer's in particular, are associated with disruptions of cerebrospinal fluid (CSF) circulation in the paravascular spaces (PVS) (Iliff et al., 2012; Xie et al., 2013). Experimental studies indicate that cardiac pulsations are the key driving force for CSF flow (Mestre et al., 2018); however, modeling studies suggest that pulsations alone are inadequate to explain the CSF flow effects in the PVS surrounding descending arteries (Asgari et al., 2016; Sharp et al., 2019). Other mechanisms such as respiration or vasomotion have been proposed as alternative drivers (Vinje et al., 2019; van Veluw et al., 2020). Recently, anatomists have noted that several of the deep suboccipital muscles, which span from the cranial-most vertebrae to the caudal surface of the skull, also have direct attachments on the dura (Scali et al., 2013). Although best known in humans (Kahkeshani and Ward, 2012), this connection has also been described in birds (Okoye et al., 2018), whales (Liu et al., 2018), turtles (Huangfu et al., 2019) and crocodiles (Zhang et al., 2016); this anatomical link is now referred to as the myodural bridge. Researchers have speculated that contraction of the muscles of the myodural bridge could lead to localized subdural negative pressure, which could alter CSF flow (Zheng et al., 2017).

In the American alligator [*Alligator mississippiensis* (Daudin 1802)] the cervical vertebrae include the axis (C2) with its elongate spinous process, the smaller atlas (C1), and an additional wedge of bone (the proatlas) which is located dorsally between the supraoccipital of the skull and the atlas. The proatlas does not encircle the spinal cord, nor does it have a bony articulation with either the skull or C1; the connective tissue surrounding the proatlas renders it more mobile than the cervical vertebrae. The cervical axial muscles of *A. mississippiensis* include the large, superficial, spinalis (Fig. 1). Reflection or removal of the spinalis exposes the suboccipital muscles, the rectus capitis posterior minor and the rectus capitis posterior major. Both of these muscles originate from C2; the minor also has an extensive origin on C1 and the proatlas. The suboccipital muscles course cranially with a slight lateral deflection to insert onto the medial (minor) and lateral (major) portions of the otoccipital bone. In addition to these attachments on the skull, micro-CT analysis clearly demonstrates that in *A. mississippiensis*, there is a direct connective tissue link between the suboccipital muscles and the spinal dura; this connection is the myodural bridge (Fig. 1B). This study was undertaken to provide a direct experimental test of the hypothesis that the myodural bridge influences the circulation of the CSF.

MATERIALS AND METHODS

Seven live sub-adult (158–192 cm total length) American alligators (*A. mississippiensis*) were obtained from the Louisiana Department of Wildlife and Fisheries. The animals were housed communally in a 29 m^2 facility that featured three submerging ponds, natural light and artificial lights on a 12 h light:12 h dark cycle. The facility was maintained at 30–33°C; warm water rain showers were provided every 20 min, which helped maintain the facility at >75% relative humidity. The alligators were maintained on a diet of previously frozen adult rats. The husbandry and use of the live alligators followed all applicable federal guidelines, and was approved by the IACUC of A.T. Still University (Protocols #209 and #217).

When an individual animal was removed from the enclosure, it was caught by noosing, its jaws taped shut around a bite pad using vinyl tape, and its fore and hind limbs taped in a retracted position. The alligator was then placed on a stiff board (244×28×3.8 cm thick), which exceeded the maximum width and length of the alligators used for this study. Six 2.5-cm-wide heavy duty straps (Northwest Tarp and Canvas; Bellingham, WA, USA) were used to secure the alligator to the board; the straps were tight enough to minimize movement of the animal but not tight enough to impede ventilation or circulation.

With the alligator's mouth held open by the bite pad, a laryngoscope was used to depress the gular valve and expose the glottis. A cuffed endotracheal tube was inserted into the larynx and

[1]Department of Anatomy, Kirksville College of Osteopathic Medicine, A.T. Still University, Kirksville, MO 63501, USA. [2]Department of Behavioral Neuroscience, Kirksville College of Osteopathic Medicine, A.T. Still University, Kirksville, MO 63501, USA. [3]Department of Mathematics, University of Oslo, 0851 Oslo, Norway. [4]Department of Family Medicine, Kirksville College of Osteopathic Medicine, A.T. Still University, Kirksville, MO 63501, USA.

*Author for correspondence (byoung@atsu.edu)

B.A.Y., 0000-0002-0988-7731

Received 10 June 2020; Accepted 11 October 2020

Journal of Experimental Biology (2020) 223, jeb230896. doi:10.1242/jeb.230896

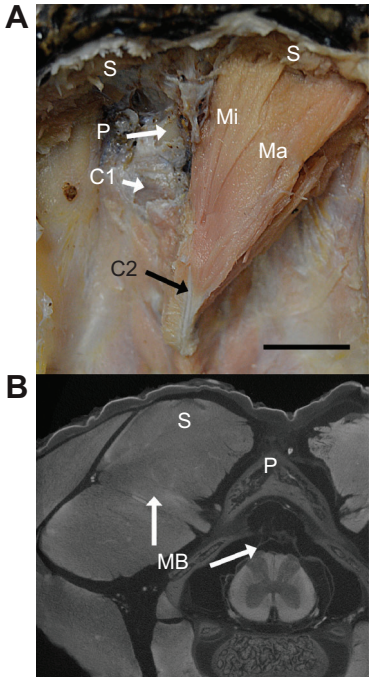

Fig. 1. Morphology of the myodural bridge of *Alligator mississippiensis*. (A) Dissection of a preserved specimen. Scale bar: 2 cm. (B) Transverse section from a micro-CT series. C1, first cervical vertebra (atlas); C2, second cervical vertebra (axis); Ma, rectus capitis posterior major; MB, myodural bridge; Mi, rectus capitis posterior minor; P, proatlas; S, spinalis (removed).

connected to a custom anesthesia system that included a ventilator pump (Harvard Apparatus, Holliston, MA, USA), Vaporstick anesthesia machine (Surgivet, Saint Paul, MN, USA), isoflurane vaporizer (Surgivet) and Capnomac Ultima respiratory gas monitor (Datex-Engstrom, Bismark, ND, USA). The alligators were maintained on a steady ventilatory pattern of 6 or 8 breaths per minute (depending on size), each with a tidal volume of 500 ml. Anesthetic induction was accomplished using 5% isoflurane; once a surgical plane of anesthesia was established, the animal was maintained on 2–3% isoflurane depending on the response of the individual alligator.

A stainless steel surgical burr was used to bore an approximately 4-mm-diameter portal through the sagittal midline of the skull just caudal to the orbits. This allowed direct exposure of the dura mater; a small incision in the dura was used to inset a segment of PE tubing into the subarachnoid space. The PE tubing was connected to a P23AA fluid pressure transducer (Statham; Gould Inc., Oxnard, CA, USA), both of which were filled with reptilian Ringer's solution (Barfuss and Dantzler, 1976). The pressure transducer was mounted to the board at a fixed site immediately adjacent to and level with the alligator's head. The implantation of the PE tubing was snug enough that no CSF leakage was observed, yet the functionality of the coupling was evident by the (pressure-driven) movement of the CSF along a distance of the PE tubing. The pressure transducer was coupled to a P122 preamplifier (GRASS, Natus Medical, Pleasanton, CA, USA). In four of the alligators, a second surgical exposure was made to the vertebral column between the forelimbs. The exposure was deep enough to enable the implantation of a second PE catheter into the subdural space surrounding the spinal cord; this second implantation site was approximately 12 cm caudal to the implantation site in the skull. The second pressure catheter was connected to a second P23AA pressure transducer and PI22 preamplifier.

An additional surgical window was used to expose the suboccipital muscles on one side of the vertebral column; this exposure was roughly equidistant (rostral–caudal) between the two implanted CSF pressure catheters. A hands-free bipolar stimulating probe was positioned on the surface of the rectus capitis posterior minor and stimuli provided by a S88 stimulator (GRASS). The muscle was induced to contract by applying either a twitch (1.0 V, 10 ms duration) or train (1.0 V, 10 ms duration, 60 pps) stimuli; both stimuli induced visible contraction of the suboccipital muscles. Since the full stimulation protocol was being performed twice (see below), tetanic contractions were avoided to minimize muscle fatigue; the potential for a graded response was explored by using both twitch and train stimuli. The CSF pressure and synced output from the muscle stimulator were recorded simultaneously (at 5.0 kHz) using the MiDas data acquisition system (Xcitex, Woburn, MA, USA). The CSF pressure transducers were individually calibrated following each experiment. The recorded signals were quantified using the MiDas software.

The alligator's scalation was reflected contralateral to the exposed suboccipital muscles, to facilitate imaging of the spinal canal using ultrasonography. The cranial pressure catheter was disconnected from the pressure transducer and used to introduce into the CSF a suspension of approximately 2.0×10^9 artificial (sulfur hexafluoride) microspheres in 5 ml of saline (Lumason; Bracco Diagnostics, Monroe Township, NJ, USA). Doppler ultrasonographic records of CSF flow were quantified using an ultrasonography machine (Mindray M7; Nanshan, Shenzhen, P.R. China). A linear array probe (Mindary L12-4) was placed contralateral to the exposed suboccipital muscles and pulsed-wave Doppler ultrasonography used to detect the spread of the introduced microspheres in the CSF. Once the microspheres had adequately dispersed (defined as when the pulsed-wave Doppler ultrasonography could detect the pulsatile waves in the CSF), the stimulation protocol of the suboccipital muscles described above was repeated. Each stimulation trial included two controls, one with the stimulator free of the alligator's body and the second with skeletal muscle away from the myodural bridge stimulated; across all of the experiments, neither control caused a change in CSF pressure or flow velocity (data not shown).

Peak CSF pressure for each stimulus was quantified relative to the resting baseline for that data trace; if no clear baseline was evident, the stimulus trial was not used. Fifteen twitch and 15 train CSF pressures were quantified; at least two twitch and two train pressure values were collected from each of the seven alligators. CSF flow velocity for each stimulus was quantified relative to the internally calibrated zero baseline of the ultrasonography machine. Fifteen twitch and six train CSF velocities were quantified; three twitch and at least one train flow value were collected from each of five alligators (flow data was not collected from the other two alligators). For both the pressure and flow data, the resting, twitch and train values were compared using MANOVA. Subsequent Bonferroni *post hoc* significance testing was performed using a threshold of $P<0.01$.

The alligator's subarachnoid space was modelled as a dynamic space between two cylinders (Tithof et al., 2019). Poiseuille's law was used to explore the relationship between CSF pressure and velocity, as well as diameter change:

$$\text{CSF velocity} = \frac{\Delta\text{CSF pressure}}{4\mu[(R_1^2-r^2)+(R_2^2-R_1^2)\times(\log[r/R_1]/\log[R_2/R_1])]}. \quad (1)$$

Anatomical values derived from MRI of one of the *A. mississippiensis* specimens were as follows: R_1 (spinal cord

Journal of Experimental Biology (2020) 223, jeb230896. doi:10.1242/jeb.230896

radius)=5 mm and R_2 (dura sheath radius)=6.5 mm. For this application, r would be the radius to the center of the subarachnoid space or 5.75 mm. We used 0.7 mPa s (the value for water) for μ, and 0.1 Pa mm^{-1} for the CSF pressure change which acted over the length of the myodural bridge, which was 35 mm.

RESULTS AND DISCUSSION

The CSF had a mean resting pressure of 533±22.7 Pa (mean±s.d.). Application of a single twitch stimulus (Fig. 2) reduced the pressure to a mean of 460±10.7 Pa, application of a train stimulus resulted in greater reduction in the CSF pressure (380±33.3 Pa). MANOVA revealed significant differences in CSF pressure following stimulation of the suboccipital muscles (2 d.f., F=93.8, P<0.0001). Bonferroni *post hoc* analysis (using a threshold of P<0.01) revealed that the two patterns of electrical stimulation were significantly different from the resting level, and from each other (Fig. 2C).

The CSF had a mean resting flow velocity of 3.3±0.65 cm s^{-1}; twitch stimuli (Fig. 3A) caused an increase in CSF flow (4.7±1.1 cm s^{-1}). A similar increase was observed during train stimuli (5.2±2.5 cm s^{-1}); the higher train mean value, and the large standard deviation, result from one trial which produced CSF flow velocity of over 10 cm s^{-1}. MANOVA revealed significant differences in CSF flow velocity following stimulation of the suboccipital muscles (2 d.f., F=8.93, P=0.0006). Bonferroni *post hoc* analysis (using a threshold of P<0.01) revealed that both stimulus conditions were significantly different from the resting level, but that the twitch and train stimuli did not produce significantly different levels of CSF flow velocity (Fig. 3B).

In the present study of *A. mississippiensis*, CSF pressure and flow were analyzed separately, and both analyses demonstrated that activation of the myodural bridge resulted in significant changes in the CSF circulation. The CSF pressure (460 Pa) and flow (4.7 cm s^{-1}) after twitch activation of the myodural bridge are similar to what have been observed (Enzmann and Pelc, 1991; Quigley et al., 2004) in studies of the human cervical region (which is similar in size and general morphology to that of the alligator). Poiseuille's law reveals that the magnitude of the CSF pressure and velocity reported herein could be achieved if the myodural bridge expanded the dura by as little as 0.2 mm. Xu et al. (2016) used magnetic resonance imaging to document that rotation of the head influenced flow patterns of the CFS, but did not document the contractile activity of the suboccipital muscles, and therefore could not directly demonstrate the influence of the myodural bridge.

The suboccipital muscles are a common feature of terrestrial vertebrates, where they function to rotate the skull in the horizontal and vertical planes (Corneil et al., 2001). As several workers have noted (Zheng et al., 2017; Dou et al., 2019), the ubiquity of head movements, both subtle and pronounced, suggest that the myodural bridge may exert a regular influence on CSF flow. More specifically, the myodural bridge has been hypothesized to function as a CSF 'pump' (Zheng et al., 2014); the term pump implies a unidirectional flow, which has not been observed in the cervical region, or CSF flow in general (Hoffmann et al., 2000;

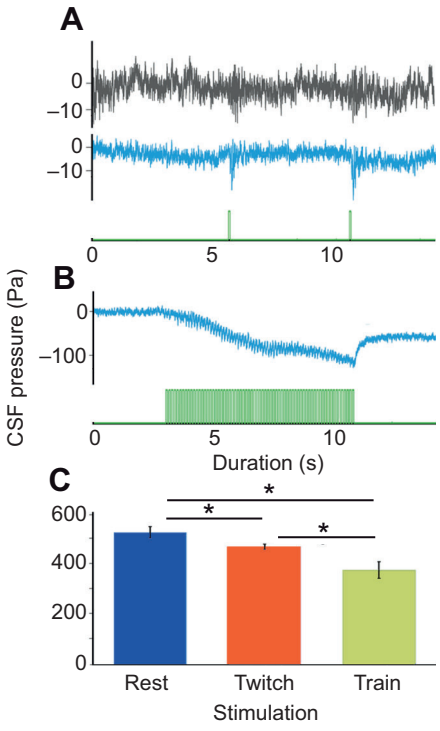

Fig. 2. The influence of stimulation of the suboccipital muscles on CSF pressure. (A) Raw data traces showing simultaneously recorded cranial CSF pressure (grey), spinal CSF pressure (blue), and muscle twitch stimulation signal (green). (B) Simultaneously recorded spinal CSF pressure (blue) and muscle train stimulation (green). (C) Mean and s.d. CSF pressures recorded at rest, during twitch stimulation and during train stimulation; 15 twitch and 15 train stimuli were compared, with at least 2 taken from each of the 7 alligators. Significant differences are indicated by the horizontal lines and asterisks (Bonferroni *post hoc* values as follows: control vs. twitch, P=6.82e^{-5}; control vs. train, P=7.03e^{-13}; twitch vs. train, P=1.49e^{-11}).

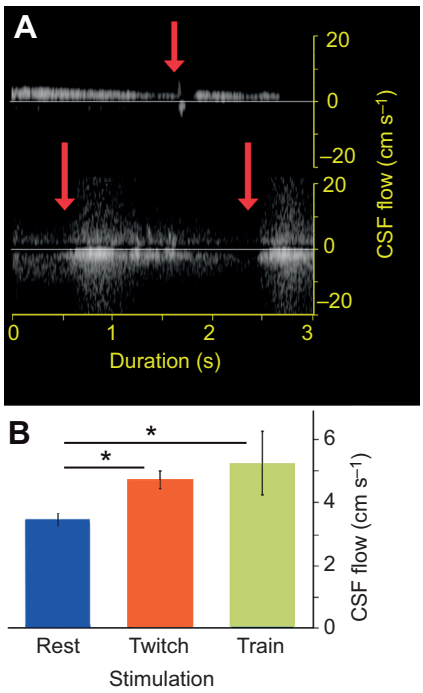

Fig. 3. The influence of stimulation of the suboccipital muscles on CSF flow. (A) Doppler ultrasonography images during twitch (upper arrow) and train (lower arrow) stimulations. The ultrasound records the flow of the artificial microspheres as the negative light traces. (B) Mean and s.d. CSF flows recorded at rest, during twitch stimulation and during train stimulation; 15 twitch and 6 train stimuli were compared, with 3 twitches and at least 1 train taken from each of 5 alligators. Significant differences are indicated by the horizontal lines and asterisks (Bonferroni *post hoc* values as follows: control vs. twitch, P=0.0047; control vs. train, P=0.0043; twitch vs. train, P=1.11).

Geregele et al., 2019). It may be more appropriate to say that the significant decrease in CSF pressure produced by the myodural bridge could alter the complex cyclic CSF flow patterns that occur at the level of the foramen magnum (Hentschel et al., 2010). Disruptions of the cervical CSF flow patterns have been associated with syringomyelia (Pinna et al., 2000; Chang and Nakagawa, 2003) and Chiari malformations (Hoffmann et al., 2000; Martin et al., 2013). The anatomical position and action of the myodural bridge suggest that it could dynamically tune the compliance of the cervical spinal region; changes in compliance play a critical role in the balance between intracranial pressure and venous (hydrostatic) pressure (Holmlund et al., 2017; Gehlen et al., 2017).

Perspectives on the meninges have been shifting (Dasgupta and Jeong, 2019): although once seen as a passive protective sheath, the meninges are now appreciated as integrally involved in a variety of critical processes including neural development (Siegenthaler and Pleasure, 2011) and repair (Decimo et al., 2012). The present study offers the first experimental evidence that the meninges are also a dynamic, rather than static, tissue. The pressure and pulsatility of human CSF is dynamically variable (Kasprowicz et al., 2016); the magnitude and shape of each CSF pulsation is largely due to the cardiac cycle (Czosnyka and Pickard, 2004). There are also slower cycles of CSF flow driven by vasomotion of the cerebral arteries and this vasomotor flow appears to play a key role in metabolic exchange with the neural tissue (Carare et al., 2020; van Veluw et al., 2020). We hypothesize that the myodural bridge functions at a frequency closer to that of vasomotion (rather than the cardiac cycle), and that it may function in distributing the CSF between the cranial and spinal subarachnoid spaces.

The CSF can be generated and eliminated in several ways: while the relative contributions of these different mechanisms remain unclear (Wagshul et al., 2011), there are multiple lines of evidence indicating that the majority of the CSF surrounding the spinal cord was produced in the brain and exited the skull at the foramen magnum (Magnaes, 1989; Geregele et al., 2019). Recent work on zebra fish embryos have shown that lateral deflection of the body, as is produced by skeletal muscle during locomotion, results in significant unidirectional flow of CSF (Olstad et al., 2019). With the evolution of tetrapods, some of the axial musculature that originally functioned in locomotion evolved into ventilatory systems (Boggs, 2002; Perry et al., 2010). Although only studied in mammals, evidence suggests that these muscular ventilatory systems are the primary agent of CSF propulsion around the spinal cord (Dreha-Kulaczewski et al., 2015). The transition from axial deflection to ventilation as the primary agent for the 'bulk flow' of CSF may be associated with a fundamental change in the nature of the CSF flow. While axial deflection is associated with unidirectional flow, experimental analyses and biophysical modeling have shown that the bulk flow of CSF in systems driven by ventilation is complexly bi-directional with periodic vortices (Hentschel et al., 2010). The myodural bridge evolved along with the transition in ventilatory mechanics and CSF bulk flow patterns. It is worth noting that the insertion of skeletal muscle onto the dura (the myodural bridge) is always restricted to an area immediately adjacent to the foramen magnum; there have been no reports of a mid-thoracic myodural bridge (Zheng et al., 2017; Dou et al., 2019). The evolutionary confluence of ventilatory CSF propulsion, increased complexity of CSF bulk flow and the evolution of a myodural bridge all suggest that the myodural bridge functions to promote the bulk flow of CSF between the cranium and the spinal canal, presumably by episodically disrupting the CSF circulatory patterns.

This hypothesized functional relationship between the myodural bridge, ventilatory mechanics, and the bulk flow patterns of the CSF suggests a variety of functional tests. Does the bulk flow pattern of CSF change in amphibians that metamorphose from an early aquatic gill-breathing stage that locomotes through lateral deflection, to a later stage characterized by limbed locomotion and lung-based ventilatory mechanics? In tetrapods that combine lateral undulation with limbed locomotion, do the ventilatory mechanics have as great an influence on CSF flow patterns as in forms with less lateral undulation? Is the bulk flow pattern of CSF different among secondarily apodal tetrapods, which have re-emphasized lateral undulation, compared with that in closely related limbed taxa? Zheng et al. (2017) proposed that the similar anatomical features found in the myodural bridge indicated a shared functional role related to CSF flow, which is a hypothesis supported by the current study. Variations in the dural contact area, angle of skeletal muscle contact and even the contents of epidural space would yield subtle interspecific differences in the nature of the myodural bridge's influence on CSF flow. Far greater functional variation may be uncovered through comparative analyses of the myodural bridge in organisms representing different patterns of locomotor deflection and ventilatory mechanics.

Acknowledgements
The authors wish to thank Lucas Knoche, Kadi Fauble, and Whitney Oberman for their assistance during the experiments, Peter Kondrashov for his continued support, and Ruth Elsey and the Louisiana Fish and Wildlife Department.

Competing interests
The authors declare no competing or financial interests.

Author contributions
Conceptualization: B.A.Y., J.A., J.M.B., K.-A.M., R.S., T.K.; Methodology: B.A.Y., J.M.B., T.K.; Validation: B.A.Y., K.-A.M., T.K.; Formal analysis: B.A.Y., K.-A.M., T.K.; Investigation: B.A.Y., T.K.; Resources: J.M.B.; Data curation: B.A.Y.; Writing - original draft: B.A.Y.; Writing - review & editing: J.A., J.M.B., K.-A.M., R.S., T.K.; Visualization: J.A.; Supervision: B.A.Y.; Project administration: B.A.Y.

Funding
This research received no specific grant from any funding agency in the public, commercial or not-for-profit sectors.

References
Asgari, M., De Zélicourt, D. and Kurtcuoglu, V. (2016). Glymphatic solute transport does not require bulk flow. *Sci. Rep.* **6**, 38635. doi:10.1038/srep38635

Barfuss, D. W. and Dantzler, W. H. (1976). Glucose transport in isolated perfused proximal tubules of snake kidney. *Am. J. Physiol.* **231**, 1716-1728. doi:10.1152/ajplegacy.1976.231.6.1716

Boggs, D. F. (2002). Interactions between locomotion and ventilation in tetrapods. *Comp. Biochem. Physiol: A Mol. Integr. Physiol.* **133**, 269-288. doi:10.1016/S1095-6433(02)00160-5

Carare, R. O., Aldea, R., Bulters, D., Alzetani, A., Birch, A. A., Richardson, G. and Weller, R. O. (2020). Vasomotion drives periarterial drainage of Aβ from the brain. *Neuron* **105**, 400-401. doi:10.1016/j.neuron.2020.01.011

Chang, H. S. and Nakagawa, H. (2003). Hypothesis on the pathophysiology of syringomyelia based on simulation of cerebrospinal fluid dynamics. *J. Neurol. Neurosurg. Psychiatry* **74**, 344-347. doi:10.1136/jnnp.74.3.344

Corneil, B. D., Olivier, E., Richmond, F. J. R., Loeb, G. E. and Munoz, D. P. (2001). Neck muscles in the rhesus monkey. II. Electromyographic patterns of activation underlying postures and movements. *J. Neurophysiol.* **86**, 1729-1749. doi:10.1152/jn.2001.86.4.1729

Czosnyka, M. and Pickard, J. D. (2004). Monitoring and interpretation of intracranial pressure. *J. Neurol. Neurosurg. Psychiatry* **75**, 813-821. doi:10.1136/jnnp.2003.033126

Dasgupta, K. and Jeong, J. (2019). Developmental biology of the meninges. *Genesis* **57**, e23288. doi:10.1002/dvg.23288

Decimo, I., Fumagalli, G., Berton, V., Krampera, M. and Bifari, F. (2012). Meninges: from protective membrane to stem cell niche. *Am. J. Stem Cells* **1**, 92-105.

Dou, Y.-R., Zheng, N., Gong, J., Tang, W., Okoye, C. S., Zhang, Y., Chen, Y.-X., Zhang, Y., Pi, S.-Y., Qu, L.-C. et al. (2019). Existence and features of the myodural bridge in *Gallus domesticus*: indication of its important physiological function. *Anat. Sci. Inter.* **94**, 184-191. doi:10.1007/s12565-018-00470-2

Dreha-Kulaczewski, S., Joseph, A. A., Merboldt, K.-D., Ludwig, H.-C., Gärtner, J. and Frahm, J. (2015). Inspiration is the major regulator of human CSF flow. *J. Neurosci.* **35**, 2485-2491. doi:10.1523/JNEUROSCI.3246-14.2015

Enzmann, D. R. and Pelc, N. J. (1991). Normal flow patterns of intracranial and spinal cerebrospinal fluid defined with phase-contrast cine MR imaging. *Radiology* **178**, 467-474. doi:10.1148/radiology.178.2.1987610

Gehlen, M., Kurtcuoglu, V. and Schmid Daners, M. (2017). Is posture-related craniospinal compliance shift caused by jugular vein collapse? A theoretical analysis. *Fluids Barriers CNS* **14**, 5. doi:10.1186/s12987-017-0053-6

Geregele, L., Baledent, O., Manet, R., Lalou, A., Barszcz, S., Kasprowicz, M., Smielewski, P., Pickard, J., Czosnyka, M. and Czosnyka, Z. (2019). Dynamics of cerebrospinal fluid: From theoretical models to clinical applications. In *Biomechanics of the Brain* (ed. K. Miller), pp. 181-214. Switzerland: Springer.

Hentschel, S., Mardal, K.-A., Løvgren, A. E., Linge, S. and Haughton, V. (2010). Characterization of cyclic CSF flow in the foramen magnum and upper cervical spinal canal with MR flow imaging and computational fluid dynamics. *Am. J. Neuroradiol.* **31**, 997-1002. doi:10.3174/ajnr.A1995

Hoffmann, E., Warmuth-Metz, M., Bendszus, M. and Solymosi, L. (2000). Phase-contrast MR imaging of the cervical CSF and spinal cord: volumetric motion analysis in patients with Chiari I malformation. *Am. J. Neurorad.* **21**, 151-158.

Holmlund, P., Johansson, E., Qvarlander, S., Wåahlin, A., Ambarki, K., Koskinen, L.-O. D., Malm, J. and Eklund, A. (2017). Human jugular vein collapse in the upright posture: implications for postural intracranial pressure regulation. *Fluids Barriers CNS* **14**, 17. doi:10.1186/s12987-017-0065-2

Huangfu, Z., Zhang, X., Sui, J.-Y., Zhao, Q.-Q., Yuan, X.-Y., Li, C., Dou, Y.-R., Tang, W., Du, M.-L., Zheng, N. et al. (2019). Existencia del Puente Miodural en Trachemys scripta elegans: indicacion de su importante funcion fisiologica. *Int. J. Morphol.* **37**, 1353-1360. doi:10.4067/S0717-95022019000401353

Iliff, J. J., Wang, M., Liao, Y., Plogg, B. A., Peng, W., Gundersen, G. A., Benveniste, H., Vates, G. E., Deane, R., Goldman, S. A. et al. (2012). A paravascular pathway facilitates CSF flow through the brain parenchyma and the clearance of interstitial solutes, including amyloid β. *Sci. Transl. Med.* **4**, 147ra111. doi:10.1126/scitranslmed.3003748

Kahkeshani, K. and Ward, P. J. (2012). Connection between the spinal dura mater and suboccipital musculature: Evidence for the myodural bridge and a route for its dissection — a review. *Clini. Anat.* **25**, 415-422. doi:10.1002/ca.21261

Kasprowicz, M., Lalou, D. A., Czosnyka, M., Garnett, M. and Czosnyka, Z. (2016). Intracranial pressure, its components and cerebrospinal fluid pressure-volume compensation. *Acta Neurol. Scand.* **134**, 168-180. doi:10.1111/ane.12541

Liu, P., Li, C., Zheng, N., Yuan, X., Zhou, Y., Chun, P., Chi, Y., Gilmore, C., Yu, S. and Sui, H. (2018). The myodural bridges' existence in the sperm whale. *PLOS ONE* **13**, e0200260. doi:10.1371/journal.pone.0200260

Magnæs, B. (1989). Clinical studies of cranial and spinal compliance and the craniospinal flow of cerebrospinal fluid. *Br. J. Neurosurg.* **3**, 659-668. doi:10.3109/02688698908992689

Martin, B., Kalata, W., Shaffer, N., Fischer, P., Luciano, M. and Loth, F. (2013). Hydrodynamic and longitudinal impedance analysis of cerebrospinal fluid dynamics at the craniovertebral junction in type I Chiari malformation. *PLoS ONE* **8**, e75335. doi:10.1371/journal.pone.oo75335

Mestre, H., Tithof, J., Du, T., Song, W., Peng, W., Sweeney, A. M., Olveda, G., Thomas, J. H., Nedergaard, M. and Kelley, D. H. (2018). Flow of cerebrospinal fluid is driven by arterial pulsations and is reduced in hypertension. *Nat. Commun.* **9**, 4878. doi:10.1038/s41467-018-07318-3

Okoye, C. S., Zheng, N., Yu, S.-B. and Sui, H.-J. (2018). The myodural bridge in the common rock pigeon (*Columbia livia*): morphology and possible physiological implications. *J. Morphol.* **279**, 1524-1531. doi:10.1002/jmor.20890

Olstad, E. W., Ringers, C., Hansen, J. N., Wens, A., Brandt, C., Wachten, D., Yaksi, E. and Jurisch-Yaksi, N. (2019). Ciliary beating compartmentalizes cerebrospinal fluid flow in the brain and regulates ventricular development. *Curr. Biol.* **29**, 229-241.e6 doi:10.1016/j.cub.2018.11.059

Perry, S. F., Similowski, T., Klein, W. and Codd, J. R. (2010). The evolutionary origin of the mammalian diaphragm. *Respir. Physiol. Neurobiol.* **171**, 1-16. doi:10.1016/j.resp.2010.01.004

Pinna, G., Alessandrini, F., Alfieri, A., Rossi, M. and Bricolo, A. (2000). Cerebrospinal fluid flow dynamics study in Chiari I malformation: implications for syrinx formation. *Neurosurg. Focus* **8**, E3. doi:10.3171/foc.2000.8.3.3

Quigley, M. F., Iskandar, B., Quigley, M. A., Nicosia, M. and Haughton, V. (2004). Cerebrospinal fluid flow in foramen magnum: Temporal and spatial patterns at MR imaging in volunteers and in patients with Chiari I malformation. *Radiology* **232**, 229-236. doi:10.1148/radiol.2321030666

Scali, F., Pontell, M. E., Enix, D. E. and Marshall, E. (2013). Histological analysis of the rectus capitis posterior major's myodural bridge. *Spine J.* **13**, 558-563. doi:10.1016/j.spinee.2013.01.015

Sharp, M. K., Carare, R. O. and Martin, B. A. (2019). Dispersion in porous media in oscillatory flow between flat plates: Applications to intrathecal, periarterial and paraarterial solute transport in the central nervous system. *Fluids Barriers CNS* **16**, 13. doi:10.1186/s12987-019-0132-y

Siegenthaler, J. A. and Pleasure, S. J. (2011). We have got you 'covered': how the meninges control brain development. *Curr. Opin. Genet. Dev.* **21**, 249-255. doi:10.1016/j.gde.2010.12.005

Tithof, J., Kelley, D. H., Mestre, H., Nedergaard, M. and Thomas, J. H. (2019). Hydraulic resistance of periarterial spaces in the brain. *Fluids Barriers CNS* **16**, 19. doi:10.1186/s12987-019-0140-y

van Veluw, S. J., Hou, S. S., Calvo-Rodriguez, M., Arbel-Ornath, M., Snyder, A. C., Frosch, M. P., Greenberg, S. M. and Bacskai, B. J. (2020). Vasomotion as a driving force for paravascular clearance in the awake mouse brain. *Neuron* **105**, 549-561.e5. doi:10.1016/j.neuron.2019.10.033

Vinje, V., Ringstad, G., Lindstrøm, E. K., Valnes, L. M., Rognes, M. E., Eide, P. K. and Mardal, K.-A. (2019). Respiratory influence on cerebrospinal fluid flow – a computational study based on long-term intracranial pressure measurements. *Sci. Rep.* **9**, 9732. doi:10.1038/s41598-019-46055-5

Wagshul, M., Eide, P. and Madsen, J. (2011). The pulsating brain: a review of experimental and clinical studies of intracranial pulsatility. *Fluids Barriers CNS* **8**. https://doi.org/10.1186/2045-8118-8-5.

Xie, L., Kang, H., Xu, Q., Chen, M. J., Liao, Y., Thiyagarajan, M., O'Donnell, J., Christensen, D. J., Nicholson, C., Iliff, J. J. et al. (2013). Sleep drives metabolite clearance from the adult brain. *Science* **342**, 373-377. doi:10.1126/science.1241224

Xu, Q., Yu, S.-B., Zheng, N., Yuan, X.-Y., Chi, Y.-Y., Liu, C., Wang, X.-M., Lin, X.-T. and Sui, H.-J. (2016). Head movement, an important contributor to human cerebrospinal fluid circulation. *Sci. Rep.* **6**, 31787. doi:10.1038/srep31787

Zhang, J.-H., Tang, W., Zhang, Z.-X., Luan, B.-Y., Yu, S.-B. and Sui, H.-J. (2016). Connection of the posterior occipital muscle and dura mater of the Siamese crocodile. *Anat. Rec.* **299**, 1402-1408. doi:10.1002/ar.23445

Zheng, N., Yuan, X.-Y., Li, Y.-F., Chi, Y.-Y., Gao, H.-B., Zhao, X., Yu, S.-B., Sui, H.-J. and Sharkey, J. (2014). Definition of the *to be named* ligament and *Vertebrodural* ligament and their possible effects on the circulation of CSF. *PLoS ONE* **9**, e103451. doi:10.1371/journal.pone.0103451

Zheng, N., Yuan, X.-Y., Chi, Y.-Y., Liu, P., Wang, B., Sui, J.-Y., Han, S.-H., Yu, S.-B. and Sui, H.-J. (2017). The universal existence of myodural bridge in mammals: an indication of a necessary function. *Sci. Rep.* **7**, 8248. doi:10.1038/s41598-017-06863-z